JOURNAL OF THE BALKAN GEOPHYSICAL SOCIETY, Vol. 3, No 3, August 2000, p. 37-44, 13 figs.

Interpretation of gravity and aeromagnetic anomalies of the Konya Region, South Central Turkey

A. Ates[1,*] and P. Kearey[2]

[1] Ankara Üniversitesi, Jeofizik Mühendisligi Bölümü, Besevler 06100 Ankara, Turkey.
[2] Department of Earth Sciences, University of Bristol, Bristol BS8 1RJ, UK.
[*] Corresponding author: ates@science.ankara.edu.tr

(Received 7 February 2000; accepted 14 Mart 2000

Abstract: *Some 100 km southwest of Tuz Lake in central Turkey there are strong gravity and magnetic anomalies oriented in a NW-SE direction. The surface geology does not suggest a cause for the anomalies although there are some small exposures of mafic and ultramafic rocks. The gravity and aeromagnetic anomaly fields are separated into regional and residual anomalies by graphical and planar trend removal, respectively. Three-dimensional models of residual gravity and magnetic anomalies are constructed using an iterative method and depths controlled by power spectrum analysis. A density contrast of 0.5 g/cm^3 is used with the gravity model. Pseudodensity contrast ranges of 0.2-0.5 g/cm^3 are used with the magnetic models. The models constructed suggest that different bodies cause the gravity and magnetic anomalies and their bases extend no deeper than the middle of the upper crust. It is suggested that magma was injected into the upper crust at two different stages from the same location. The second stage probably commenced with the formation of high magnetite content igneous rocks when the African plate was closer to the Anatolian plate.*

Key words: *Gravity and Aeromagnetic Anomalies Interpretation, Konya Region, South Central Turkey*

GEOLOGICAL SETTING

The area studied is located between the Inner Tauride and Pan-African sutures (Fig. 1), the former being an Alpine structure and the latter Precambrian. A geological map (Fig. 2), simplified from Bingöl (1989), shows widespread Quaternary deposition in the study area. Mafic and ultramafic rocks can be seen as small outcrops. Interestingly, in the NW and SE of the region, mafic and ultramafic rocks outcrop and these appear to be elongated in a NW-SE direction. Kocyigit (1976) investigated the Ermenek (Konya) ophiolitic mélange near the south of the studied area. He suggested that the outcropping serpentinized peridotites comprise parts of the upper mantle injected upwards along cracks and mixed with deep sea deposits and other basic rocks. Temel *et al*. (1998) studied the petrological and geochemical characteristics of Cenozoic high-K calc-alkaline volcanism of the Konya region. They suggested that the Konya volcanic rocks show the effect of crustal contamination on andesitic and dacitic magma. Further, they considered that fractional crystallization of the magma took place because of the subduction of the African plate beneath the Anatolian plate during Miocene times.

The regional gravity and aeromagnetic anomalies of Turkey show strong anomalies located on [37°25'N; 32°45'E] (Ates *et al*., 1999). Gravity and aeromagnetic anomalies which cover the area of Figure 2, gridded at 2.5 km, were obtained from the General Directorate of Mineral Exploration and Research Company of Turkey (MTA). The Bouguer gravity contour map (Fig. 3) shows a large positive anomaly which is surrounded by several negative anomalies. The aeromagnetic field of the region is shown in Figure 4.

REGIONAL GRAVITY FIELD

The geological map (Fig. 2) does not show an apparent cause for the large central positive gravity anomaly. The contour map in Figure 3 demonstrates that the structure causing the anomaly seems to be superimposed on a negative regional background (Simmons, 1964). In order to determine the regional gravity field, 11 north-south and 11 east-west profiles were constructed at 11 km intervals using the data of Figure 3. The regional field on each profile was drawn and then correlated with other transecting profiles at the tie points (Simmons, 1964). This method was also used by Kearey (1978) to interpret the gravity field of the Morin Anorthosite Complex in southwest Quebec. Two

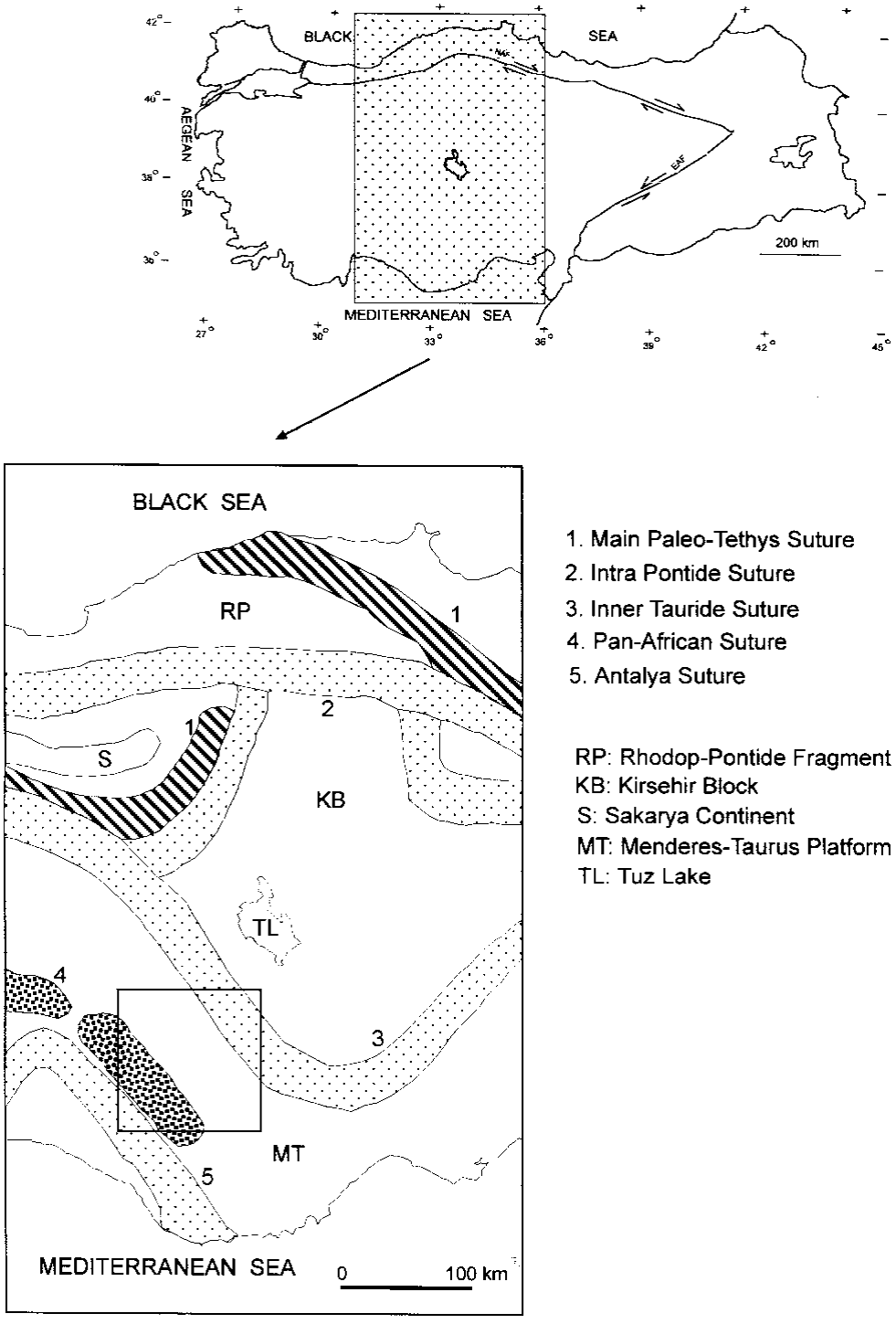

FIG. 1. Location map and regional setting of the studied area.

examples of profiles along N-S and E-W directions are given in Figure 5.

The contoured regional field (Fig. 6) is assumed to approximate the gravity field of deep sources and appears not to reflect anomalous features seen in the original gravity anomaly map of Figure 3. Contours on the regional gravity anomalies vary from -35 to -53 mGal. This result is in agreement with the observation of Ates *et al*. (1999) that most of Turkey is represented by negative gravity anomalies which reflect the isostatically thickened continental crust. The regional field (Fig. 6) also shows a broad low trending in a NW-SE

direction. A low density body located no deeper than the lower crust could cause this anomaly. It may be the root of the body causing the gravity and magnetic anomalies shown in Figures 3 and 4.

RESIDUAL GRAVITY AND AEROMAGNETIC ANOMALIES

The graphically determined regional field (Fig. 6) was gridded at 2.5 km intervals using a standard gridding routine and subtracted from the observed field at these points; the resultant residual gravity anomalies are shown in Figure 7. The surface geology does not show an obvious cause of the positive residual gravity anomalies, with the exception of some outcrops of mafic and ultramafic rocks in the northwest and southeast elongated in a NW direction. The negative anomalies surrounding the large positive anomaly appear to reflect a low density zone. A research borehole [464.853E; 4185.025N], drilled by MTA at the peak of the gravity anomaly in the NW encountered serpentinized peridotite at approximately 170 m depth from the surface. A density of 2.70 g/cm^3 was measured on a core sample of the serpentinized peridotite extracted from this borehole. This could explain the low density zone surrounding the high density body. Susceptibility measurement was also carried out on the same sample using a Scintrex SM5 susceptibility meter. The measured maximum susceptibility of the core was 1.3×10^{-3} (SI), which indicates a low magnetization.

A regional planar trend was removed from the aeromagnetic anomalies shown in Figure 4 to isolate the near surface effects (Dobrin and Savit, 1988). The residual field is shown in Figure 8. It is evident that

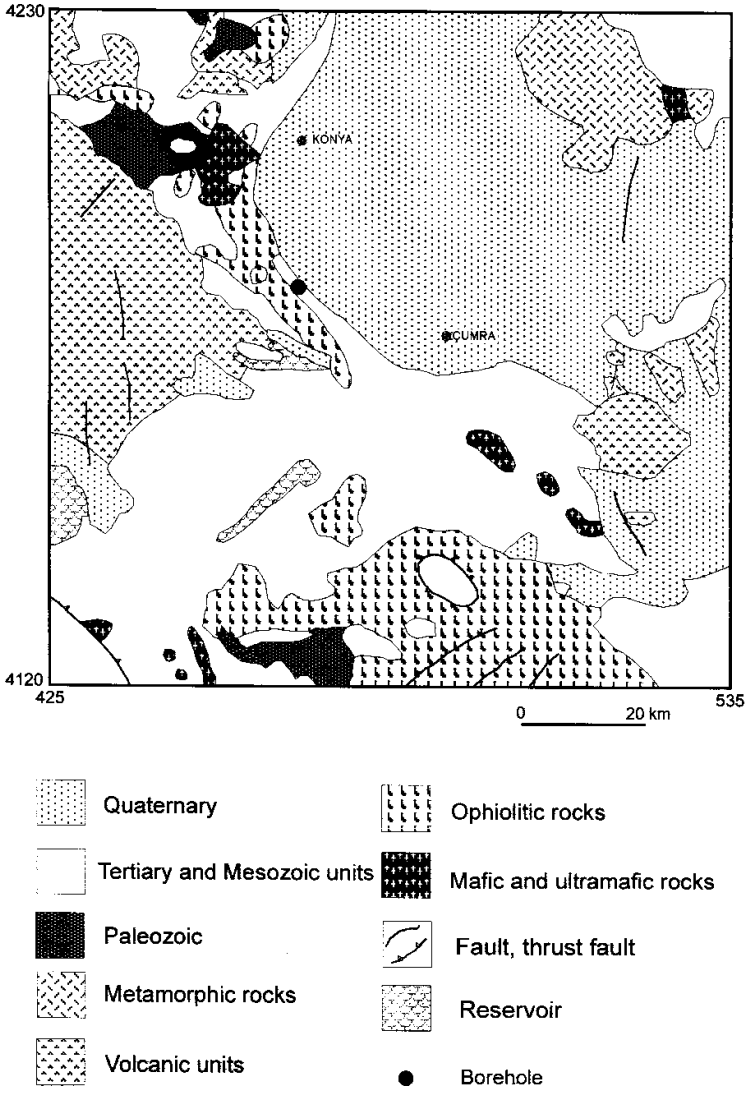

FIG. 2. Geological map of the studied area (after Bingöl, 1989).

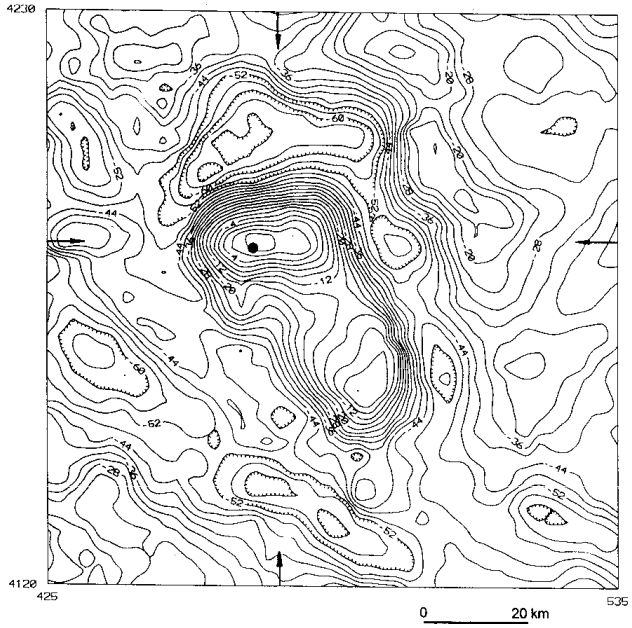

FIG. 3. Gravity anomaly map of the studied area. The contour interval is 4 mGal. The arrows mark the locations of the profiles shown in Figure 5. The solid circle shows the location of the exploratory borehole CS-1.

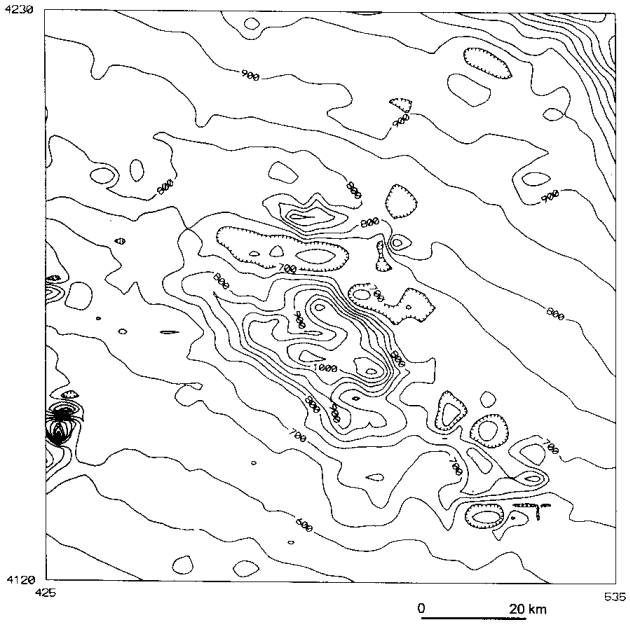

FIG. 4. Aeromagnetic anomalies of the area shown in Figure 2. The contour interval is 50 nT.

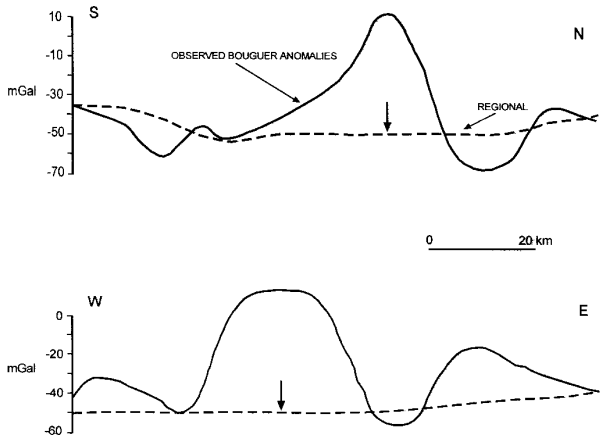

FIG. 5. Examples of north-south and east-west gravity profiles used to construct the regional field. Profile locations are shown in Figures 3 and 6. The black arrows mark the intersection of the profiles.

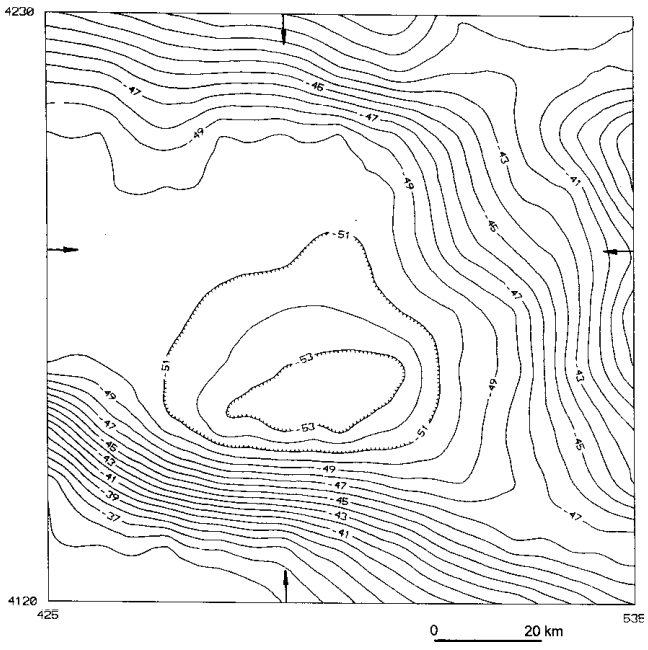

FIG. 6. Regional gravity anomalies. The contour interval is 1 mGal. The black arrows mark the profiles along which the anomaly has been plotted in Figure 5.

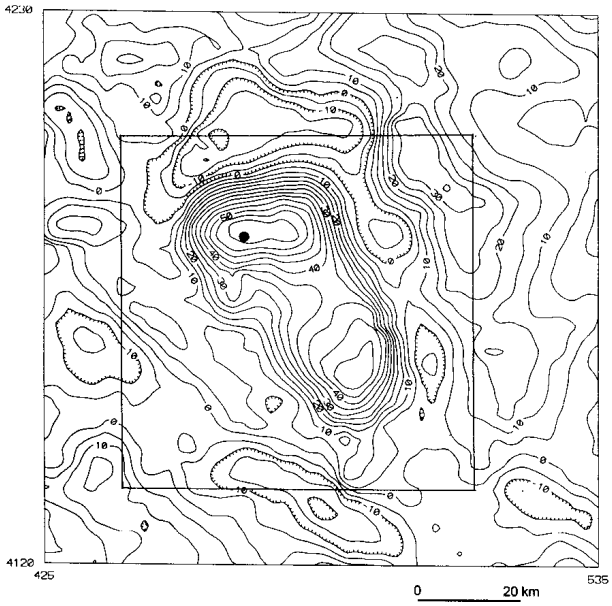

FIG. 7. Residual gravity anomalies in the studied area. The contour interval is 5 mGal. The solid lines enclose the area where the data were subjected to further processing and interpretation.

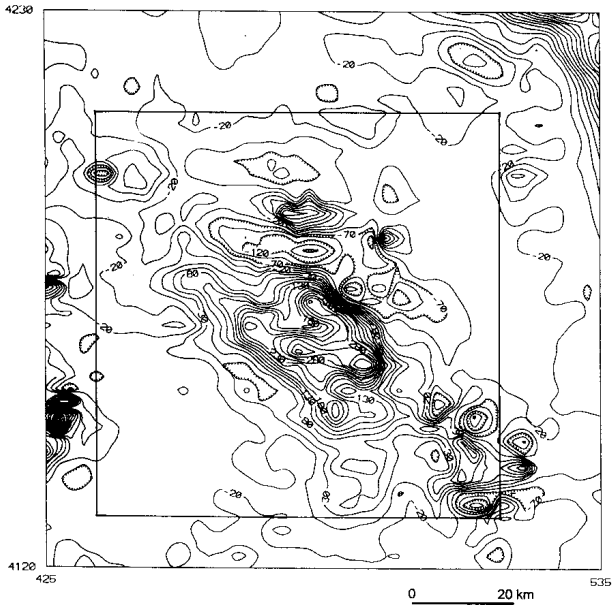

FIG. 8. Residual aeromagnetic anomalies after the removal of a planar regional trend. The contour interval is 25 nT. The solid lines delineate the area where the data were subjected to further processing.

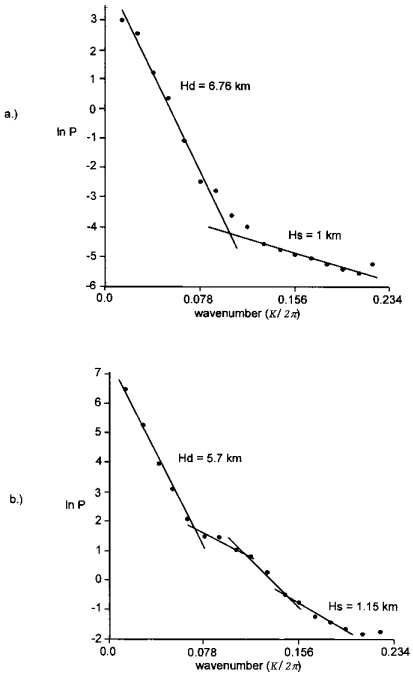

FIG. 9. **(**a) Logarithmic power spectrum obtained from the gravity anomalies of the area enclosed by the box in Figure 7. The power spectrum obtained from the residual aeromagnetic anomalies in the same area is shown in (b). Hs and Hd are the depths to the top of the shallow and deep sources, respectively.

FIG. 10. Gravity model of the Konya anomaly. The model is presented as contours on top of the model. The contour interval is 0.5 km. The density contrast is 0.5 g/cm^3. Edge effects in a narrow band are suppressed in the west, north and east.

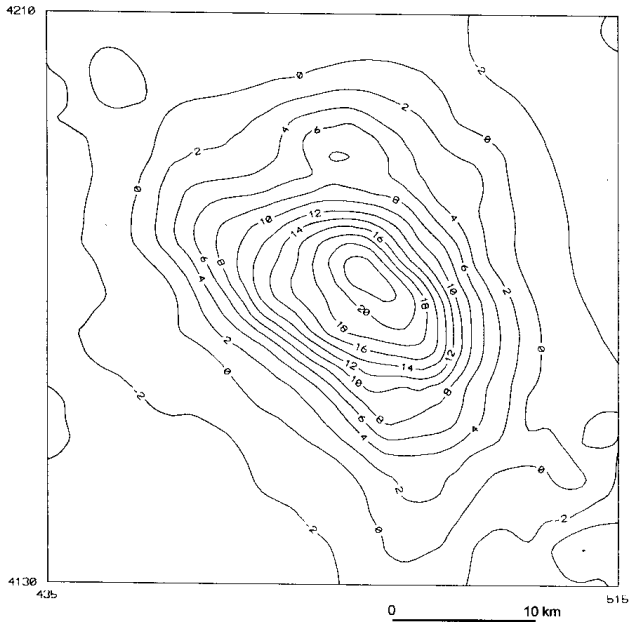

FIG. 11. Pseudogravity anomaly of the residual aeromagnetic anomaly shown enclosed in the box. The contour interval is 1 mGal.

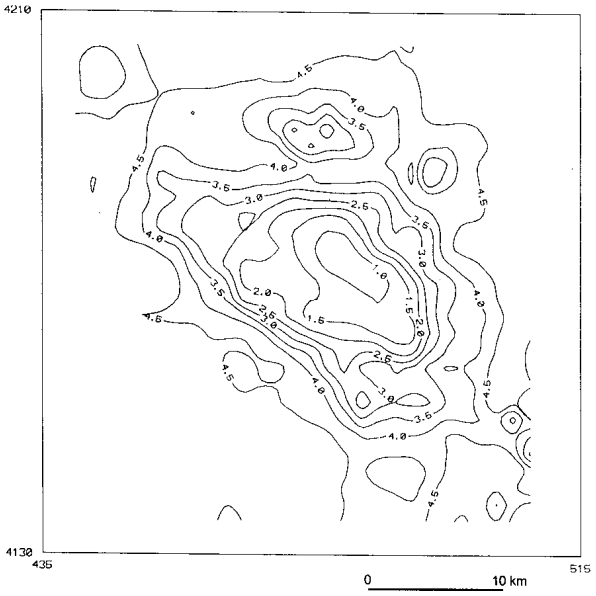

FIG. 12. Model of the Konya pseudogravity anomaly shown in Figure 11. The model is presented as contours on top of the body. The contour interval is 0.5 km. The pseudodensity contrast is 0.2 g/cm^3.

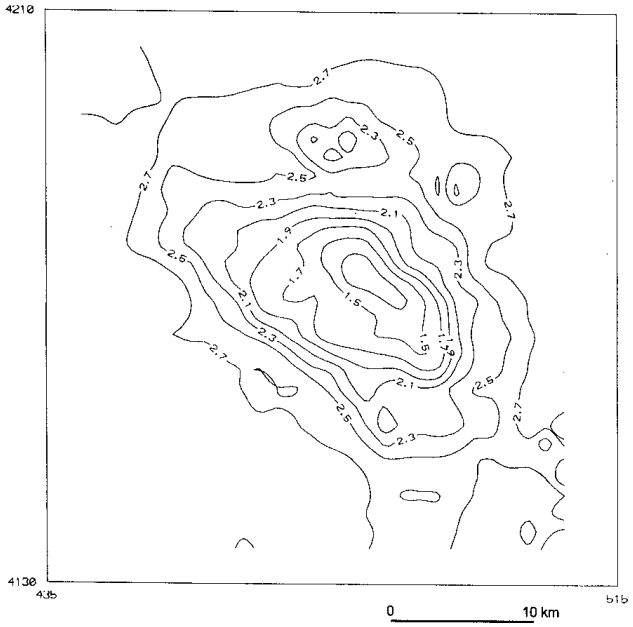

FIG. 13. Model of the Konya pseudogravity anomaly shown in Figure 11. The model is presented as contours on top of the body. The contour interval is 0.2 km. The pseudodensity contrast is 0.5 g/cm^3.

the aeromagnetic anomalies are restricted to the small area enclosed by a box in Figure 8. This box is delineated by the co-ordinates [435; 515] E and [4130; 4210] N. The overall trend of the aeromagnetic anomalies is in a NW-SE direction, but the relative locations of the positive and negative lobes suggest that the magnetization is in a N-S direction.

POWER SPECTRUM ANALYSIS

Figures 9a and 9b show the azimuthally-averaged logarithmic power spectra of the gravity and aeromagnetic anomalies of the areas shown in Figures 7 and 8, respectively. The depth to the upper surface of the deep sources is estimated to be 6.76 km from gravity data and 5.7 km from the aeromagnetic data. The estimates for the shallow sources is 1.0 km and 1.15 km inferred from the gravity and magnetic anomalies, respectively. Thus, it is quite likely that the gravity and magnetic anomalies originate from the same sources.

THREE-DIMENSIONAL INTERPRETATION OF THE RESIDUAL GRAVITY AND AEROMAGNETIC ANOMALIES

The residual anomaly of the area enclosed by the co-ordinates [4135; 4205] N and [440; 510] E was

selected for three-dimensional interpretation. The negative values surrounding the large positive anomaly were suppressed to zero for the purposes of the three-dimensional modelling. Then the residual gravity anomalies in the area were modelled using the iterative method of Cordell and Henderson (1968). In this method, an initial approximation of the causative body is calculated assuming an infinite horizontal slab at each grid point of the gravity field. The final model is constructed of vertical right rectangular prisms by modifying the first and successive models by the ratio of observed to calculated gravity field. A density contrast between the anomalous body and the host medium was set to the value of 0.5 g/cm^3. This is assumed to be the density difference between the upper mantle (3.35 g/cm^3) and the lower crust (2.85 g/cm^3). The depth of the bottom of the model was changed until the depth to the top of the model was at 1 km from the ground surface as inferred from the power spectrum analysis. The resulting three-dimensional gravity model is shown in Fig. 10.

For the same area the pseudogravity transformation of the residual aeromagnetic anomaly was performed using a computer program written by Blakely and Simpson (1986). Magnetization of induced type only was considered in this computation and the ratio of intensity of induced magnetization (J) to density (r) taken as unity. It is easier to interpret a pseudogravity anomaly than a magnetic anomaly. Figure 11 shows the pseudogravity anomaly, which was also modelled using the iterative method of the Cordell and Henderson (1968). The depth of the base of model was varied until the top of the body reached a depth of 1.15 km, as suggested by the power spectrum calculation. Two models were constructed using two different density contrasts of 0.2 g/cm^3 and 0.5 g/cm^3. The bases of the models are at 4.5 km from the surface for a density contrast of 0.2 g/cm^3 , and 2.7 km for that model of 0.5 g/cm^3 density contrast. The aeromagnetic models produced using 0.2 g/cm^3 and 0.5 g/cm^3 are shown in Figs 12 and 13, respectively. The shape of the model which was constructed for a density contrast 0.5 g/cm^3 is similar to the gravity model (Fig. 10).

DISCUSSION

The geological map of Figure 2 shows mafic and ultramafic outcrops elongated mainly in a NW-SE direction, which may be the only magnetic rocks present in the area. Similar outcrops can be seen elsewhere, NE of Tuz Lake, and all exhibited large susceptibilities while other rock formations showed small or negligible susceptibility values (Ates and Kearey, sub judice). These mafic and ultramafic rocks could be responsible for the strong magnetic and gravity anomalies. However, their dimensions and shape suggest that they cannot justify the amplitude and shape of the observed anomalies. One explanation is that a large body of mafic and ultramafic formations could be concealed under the Quaternary cover. In such a case, the gravity and magnetic models of Figures 10 and 12 show that this body is approximately 4 km thick, while the magnetic model in Figure 13 suggests that the magnetic body is approximately 1.7 km thick. The orientation of both the gravity and magnetic models is in a NW-SE direction. Depth estimates inferred by the spectral analysis also suggest that the top of the body causing the gravity anomaly is at a depth of 1 km from the surface, while the top of the magnetic source is at the depth of 1.15 km. However, detailed investigation of the gravity and magnetic models show that they are different from each other. The model inferred from the gravity data (Fig. 10) has two peaks at its NW and SE parts, which are buried at about 1-1.5 km beneath the surface. At the centre, the depth of the top of the body is about 3-3.5 km. The top of the magnetic body is at a depth of 1 km from the surface at its centre and it has a conical shape. The magnetic body seems to be situated at the top and in between the peaks of the body causing the gravity anomaly. It can thus be suggested that there are two stages of intrusion from the upper mantle into the lower and then the upper crust with different mineral compositions. The latter stage was when the African plate was closer to the Anatolian plate and it had a mafic composition. Thus, the magnetic body may be older than the gravity body, which has no magnetization. The magnetic body does not appear to exhibit a considerable amount of remanent magnetization which would reflect the anticlockwise rotation of central Turkey suggested by Sanver and Ponat (1981), Rotstein (1984) and Bilim and Ates (1999). Therefore, it may be suggested that the body causing the magnetic anomalies is young in age, perhaps formed during Oligocene times, as suggested by Ates *et al* (1997) for the intrusive bodies in SW Turkey. An alternative interpretation is that a large body was intruded into the area. Subsequently, it was altered at its base in such a way that the magnetite, which was at depth in the body, was removed.

CONCLUSIONS

In this paper, gravity and aeromagnetic anomalies and their relation to the surface geology in an area of

central Turkey were studied. Three-dimensional models of gravity and aeromagnetic data were constructed with the constraint of power spectrum depth control, and true/pseudodensity data as parameters. It was concluded from the models presented that the causative bodies were intruded into the upper crust via the lower crust from the upper mantle. Their shapes suggest two different products from the same location at different times. The second emplacement probably occurred with a magma of high magnetite content. It was also concluded that the latter stage commenced when the African plate was close to the Anatolian platelet.

ACKNOWLEDGEMENT

The authors would like to thank the editor Dr. Gregory Tsokas and referee Dr. Alexandros Stampolidis for their constructive critisisms of an earlier version of this paper. AA kindly thanks the financial support of the Ankara University, Research Fund Scheme (AFP) to this work under grant no: 97.05.01.01. The authors also thank MTA for the provision of potential field and borehole data for this study.

REFERENCES

Ates, A. and Kearey, P., 1999. Deep structure of NE Tuz Lake, Central Anatolia, from potential field, seismic, borehole and other geophysical and geological data (sub judice).

Ates, A., Kearey, P. and Tufan, S., 1999. New gravity and magnetic anomaly maps of Turkey: Geophysical Journal International, **136**, 499-502.

Ates, A., Sevinc, A., Kadioglu, Y. K. and Kearey, P., 1997. Geophysical investigations of the deep structure of the Aydin-Milas region, southwest Turkey: Evidence for the possible extension of the Hellenic Arc, Israel Journal of Earth Sciences, **46**, 29-40.

Bilim, F. and Ates, A., 1999. A computer program to estimate the source body magnetization direction from magnetic and gravity anomalies: Computers and Geosciences, **25**, 231-240.

Bingöl, E., 1989. 1:2 000 000 scale geological map of Turkey, Publication of the Mineral Research and Exploration Company of Turkey.

Blakely, R. J. and Simpson, R. W., 1986. Approximating edges of source bodies from magnetic or gravity anomalies: Geophysics, **51**, 1494-1498.

Cordell, L. and Henderson, R. G., 1968. Iterative three-dimensional solution of gravity anomaly data using a digital computer: Geophysics, **33**, 596-601.

Dobrin, M. B. and Savit, C. H., 1988. Introduction to geophysical prospecting: McGraw Hill Book Company, 867pp.

Kearey, P., 1978. A interpretation of the gravity field of the Morin Anorthosite Complex, southwest Quebec: Geological Society of America Bulletin, **89**, 467-475.

Kocyigit, A., 1976. The ophiolitic melange and other formations in the Karaman, Eremenek (Konya) region: Bulletin of the Geological Society of Turkey, **19**, 103-116.

Rotstein, Y., 1984. Counterclockwise rotation of the Anatolian block: Tectonophysics, **108**, 71-79.

Sanver, M. and Ponat, E., 1981. Kirsehir ve dolaylarina iliskin paleomanyetik bulgular, Kirsehir Masifinin rotasyonu: Istanbul Yerbilimleri, **2**, 231-238.

Temel, A., Gundogdu, M. N. and Gourgard, A., 1998. Petrological and geochemical characteristic of Cenozoic high-K calc-alkaline volcanism in Konya, central Anatolia, Turkey: Journal of Volcanology and Geothermal Research, **85**, 327-354.

Simmons, G., 1964. Gravity survey and geological interpretation, northern New York: Geological Society of America Bulletin, **75**, 81-98.